FirstPage

Pure Spin Current Injection in Hydrogenated Graphene Structures

Reinaldo Zapata-Peña[1], Bernardo S. Mendoza[1], Anatoli I. Shkrebtii[2]

[1]*Centro de Investigaciones en Óptica, León, Guanajuato 37150, México and*

[2]*University of Ontario, Institute of Technology, Oshawa, ON, L1H 7L7, Canada*

(Dated: May 19, 2017)

Lorem ipsum dolor sit amet, consectetuer adipiscing elit. Etiam lobortis facilisis sem. Nullam nec mi et neque pharetra sollicitudin. Praesent imperdiet mi nec ante. Donec ullamcorper, felis non sodales commodo, lectus velit ultrices augue, a dignissim nibh lectus placerat pede. Vivamus nunc nunc, molestie ut, ultricies vel, semper in, velit. Ut porttitor. Praesent in sapien. Lorem ipsum dolor sit amet, consectetuer adipiscing elit. Duis fringilla tristique neque. Sed interdum libero ut metus. Pellentesque placerat. Nam rutrum augue a leo. Morbi sed elit sit amet ante lobortis sollicitudin. Praesent blandit blandit mauris. Praesent lectus tellus, aliquet aliquam, luctus a, egestas a, turpis. Mauris lacinia lorem sit amet ipsum. Nunc quis urna dictum turpis accumsan semper.

I. INTRODUCTION

Lorem ipsum dolor sit amet, consectetuer adipiscing elit. Etiam lobortis facilisis sem. Nullam nec mi et neque pharetra sollicitudin. Praesent imperdiet mi nec ante. Donec ullamcorper, felis non sodales commodo, lectus velit ultrices augue, a dignissim nibh lectus placerat pede. Vivamus nunc nunc, molestie ut, ultricies vel, semper in, velit. Ut porttitor. Praesent in sapien. Lorem ipsum dolor sit amet, consectetuer adipiscing elit. Duis fringilla tristique neque. Sed interdum libero ut metus. Pellentesque placerat. Nam rutrum augue a leo. Morbi sed elit sit amet ante lobortis sollicitudin. Praesent blandit blandit mauris. Praesent lectus tellus, aliquet aliquam, luctus a, egestas a, turpis. Mauris lacinia lorem sit amet ipsum. Nunc quis urna dictum turpis accumsan semper. Lorem ipsum dolor sit amet, consectetuer adipiscing elit. Etiam lobortis facilisis sem. Nullam nec mi et neque pharetra sollicitudin. Praesent imperdiet mi nec ante. Donec ullamcorper, felis non sodales commodo, lectus velit ultrices augue, a dignissim nibh lectus placerat pede. Vivamus nunc nunc, molestie ut, ultricies vel, semper in, velit. Ut porttitor. Praesent in sapien. Lorem ipsum dolor sit amet, consectetuer adipiscing elit. Duis fringilla tristique neque. Sed interdum libero ut metus. Pellentesque placerat. Nam rutrum augue a leo.

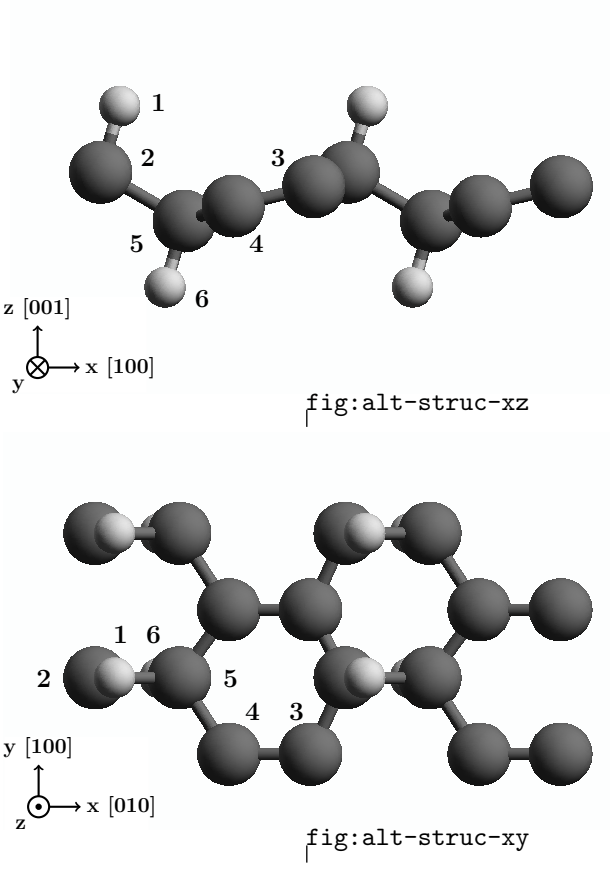

fig:alt-struc-xz

fig:alt-struc-xy

FIG. 1. Alt structure fig:alt-struc

Morbi sed elit sit amet ante lobortis sollicitudin. Praesent blandit blandit mauris. Praesent lectus tellus, aliquet aliquam, luctus a, egestas a,

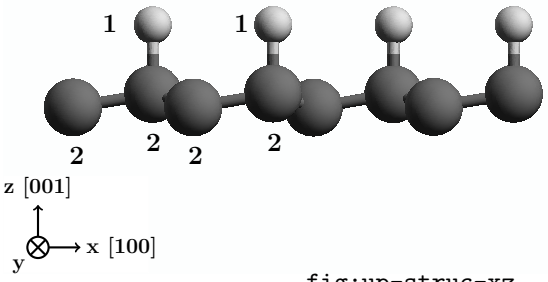

fig:up-struc-xz

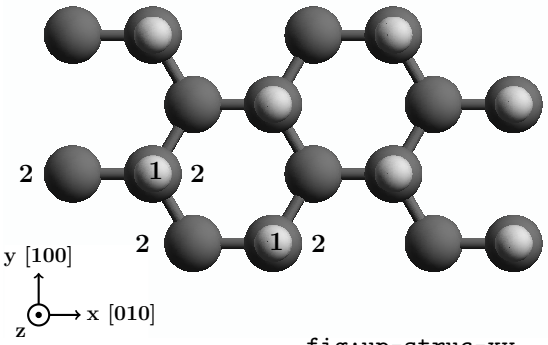

fig:up-struc-xy

FIG. 2. Up structure fig:up-struc

turpis. Mauris lacinia lorem sit amet ipsum. Nunc quis urna dictum turpis accumsan semper. Lorem ipsum dolor sit amet, consectetuer adipiscing elit. Etiam lobortis facilisis sem. Nullam nec mi et neque pharetra sollicitudin. Praesent imperdiet mi nec ante. Donec ullamcorper, felis non sodales commodo, lectus velit ultrices augue, a dignissim nibh lectus placerat pede. Vivamus nunc nunc, molestie ut, ultricies vel, semper in, velit. Ut porttitor. Praesent in sapien. Lorem ipsum dolor sit amet, consectetuer adipiscing elit. Duis fringilla tristique neque. Sed interdum libero ut metus. Pellentesque placerat. Nam rutrum augue a leo. Morbi sed elit sit amet ante lobortis sollicitudin. Praesent blandit blandit mauris. Praesent lectus tellus, aliquet aliquam, luctus a, egestas a, turpis. Mauris lacinia lorem sit amet ipsum. Nunc quis urna dictum turpis accumsan semper.

Lorem ipsum dolor sit amet, consectetuer adipiscing elit. Etiam lobortis facilisis sem. Nullam nec mi et neque pharetra sollicitudin. Praesent imperdiet mi nec ante. Donec ullamcorper, felis non sodales commodo, lectus velit ultrices augue, a dignissim nibh lectus placerat pede. Vivamus nunc nunc, molestie ut, ultricies vel, semper in, velit. Ut porttitor. Praesent in sapien. Lorem ipsum dolor sit amet, consectetuer adipiscing elit. Duis fringilla tristique neque. Sed interdum libero ut metus. Pellentesque placerat. Nam rutrum augue a leo. Morbi sed elit sit amet ante lobortis sollicitudin. Praesent blandit blandit mauris. Praesent lectus tellus, aliquet aliquam, luctus a, egestas a, turpis. Mauris lacinia lorem sit amet ipsum. Nunc quis urna dictum turpis accumsan semper.

II. THEORY

sec:theory

A. Pure spin velocity

sec:theory-pure_spin_current

The spin density injection current $\dot{K}^{\mathrm{ab}}$ with speed along direction a and spin polarization along b is defined as

$$\dot{K}(\omega) = \mu^{\mathrm{abcd}}(\omega) E^{\mathrm{c}}(\omega) E^{\mathrm{d}*}(\omega) \quad \text{eq:dotk} \tag{1}$$

where

$$\mu^{\mathrm{abcd}}(\omega) = \frac{\pi e^2}{\hbar^2} \int \frac{d^3K}{8\pi^3} \sum_{vcc'}{}' \mathrm{Re}\left[K^{\mathrm{ab}}_{cc'}(r^{\mathrm{c}}_{vc'} r^{\mathrm{d}}_{cv} + r^{\mathrm{d}}_{vc'} r^{\mathrm{c}}_{cv})\right] \delta(\omega - \omega_{cv}) \quad \text{eq:mu} \tag{2}$$

$$K^{\mathrm{ab}}_{mn} = \sum_{\ell} v^{\mathrm{a}}_{n\ell} S^{\mathrm{b}}_{\ell m} \quad \text{eq:velspi-matelem} \tag{3}$$

is the corresponding spin density injection current pseudotensor. The $'$ in the sum means that

c and c' are quasi degenerate states and the sum only covers these states.

Now we define the spin velocity, $\mathcal{V}^{\rm ab}$ as the speed at which the spin polarized in the b direction moves along the a direction when a normal incident beam reaches the xy plane with a polarization angle α. Then,

$$\begin{aligned}\mathcal{V}^{\rm ab}(\omega,\alpha) &= \frac{2}{\hbar}\frac{\mu^{\rm abxx}(\omega)E^2(\omega)\cos^2(\alpha)+\mu^{\rm abyy}(\omega)E^2(\omega)\sin^2(\alpha)+2\mu^{\rm abxy}(\omega)E^2(\omega)\cos(\alpha)\sin(\alpha)}{\xi^{\rm xx}(\omega)E^2(\omega)\cos^2(\alpha)+\xi^{\rm yy}(\omega)E^2(\omega)\sin^2(\alpha)},\\ &= \frac{2}{\hbar}\frac{\mu^{\rm abxx}(\omega)\cos^2(\alpha)+\mu^{\rm abyy}(\omega)\sin^2(\alpha)+\mu^{\rm abxy}(\omega)\sin(2\alpha)}{\xi^{\rm xx}(\omega)\cos^2(\alpha)+\xi^{\rm yy}(\omega)\sin^2(\alpha)}. \qquad \text{eq:vab}\ (4)\end{aligned}$$

For an angle $\alpha=\frac{\pi}{4}$ this expression can be reduced to

$$\mathcal{V}^{\rm ab}(\omega)=\frac{2}{\hbar}\frac{\mu^{\rm abxx}(\omega)+\mu^{\rm abyy}(\omega)+2\mu^{\rm abxy}(\omega)}{\xi^{\rm xx}(\omega)+\xi^{\rm yy}(\omega)}. \qquad \text{eq:vab-90deg}\ (5)$$

B. Fixing spin

sec:theory-fixspin

Considering that we have 2D structures, one of the options is fix the spin along the x, y, or z Cartesian coordinates. We define the magnitude of the spin velocity with spin polarization along the b direction as

$$|\mathcal{V}_{\sigma^{\rm b}}(\omega,\alpha)|=\sqrt{[\mathcal{V}^{\rm ax}(\omega,\alpha)]^2+[\mathcal{V}^{\rm ay}(\omega,\alpha)]^2}, \qquad \text{eq:vs-mag}\ (6)$$

and the angle at which the spin velocity is directed as

$$\gamma_{\rm b}(\omega,\alpha)=\tan^{-1}\left(\frac{\mathcal{V}^{\rm ay}(\omega,\alpha)}{\mathcal{V}^{\rm ax}(\omega,\alpha)}\right), \qquad \text{eq:gamma-ang}\ (7)$$

where the angle is measured in the counterclockwise direction from the positive x Cartesian coordinate.

C. Fixing velocity.

sec:theory-fixvel

In a similar way we can fix the velocity on the xy plane along x or y Cartesian coordinate and then define the magnitude of the spin velocity directed along the a direction as

$$|\mathcal{V}^{\rm a}(\omega,\alpha)|=\sqrt{[\mathcal{V}^{\rm ax}(\omega,\alpha)]^2+[\mathcal{V}^{\rm ay}(\omega,\alpha)]^2+[\mathcal{V}^{\rm az}(\omega,\alpha)]^2}., \qquad \text{eq:vv-mag}\ (8)$$

Then, the spin direction depends of the components of the previous equation and so we define the spin polar and azimuthal angles as

$$\theta_{\rm a}(\omega,\alpha)=\cos^{-1}\left(\frac{\mathcal{V}^{\rm az}(\omega,\alpha)}{|\mathcal{V}^{\rm a}(\omega,\alpha)|}\right),\quad 0\leq\theta\leq\pi, \qquad \text{eq:polar-ang}\ (9)$$

$$\varphi_{\rm a}(\omega,\alpha)=\tan^{-1}\left(\frac{\mathcal{V}^{\rm ay}(\omega,\alpha)}{\mathcal{V}^{\rm ax}(\omega,\alpha)}\right),\quad 0\leq\varphi\leq 2\pi. \qquad \text{eq:azimuthal-ang}\ (10)$$

where $\theta_{\rm a}(\omega,\alpha)$ is measured from the positive to the negative z Cartesian coordinate and $\varphi_{\rm a}(\omega,\alpha)$ is measured on the xy plane in the counterclockwise direction from the positive x Cartesian coordinate.

D. Layer-by-layer analysis.

sec:theory-layer

For a layered system we have that the total contribution of Eqns. (6) and (8) is given[1] by

$$|\mathcal{V}_{\sigma^{\rm b}}(\omega,\alpha)|=\ell_{\rm eff}\sum_{\ell=1}^{N_{\rm eff}}|\mathcal{V}_{\sigma^{\rm b}}(\ell|\omega,\alpha)| \qquad \text{eq:vs-layer}\ (11)$$

$$|\mathcal{V}^{\rm a}(\omega,\alpha)|=\ell_{\rm eff}\sum_{\ell=1}^{N_{\rm eff}}|\mathcal{V}^{\rm a}(\ell|\omega,\alpha)| \qquad \text{eq:vv-layer}\ (12)$$

Layer No.	Atom type	Position [Å] x	y	z
1	H	-0.61516	-1.42140	1.47237
2	C	-0.61516	-1.73300	0.39631
3	C	0.61516	1.73300	0.15807
4	C	0.61516	0.42201	-0.15814
5	C	-0.61516	-0.37396	-0.39632
6	H	-0.61516	-0.68566	-1.47237

TABLE I. Unit cell of *alt* structure. Layer division, atom types and positions for the *alt* structure. The structure unit cell was divided in six layers corresponding each one to atoms in different z positions. The corresponding layer atom position is depicted in Fig. 1 with the corresponding number of layer.

tab:alt-unitcell

Layer No.	Atom type	Position [Å] x	y	z
1	H	-0.61516	-1.77416	0.73196
1	H	0.61518	0.35514	0.73175
2	C	-0.61516	-1.77264	-0.49138
2	C	-0.61516	-0.35600	-0.72316
2	C	0.61516	0.35763	-0.49087

TABLE II. Unit cell of *up* structure. Layer division, atom types and positions for the *up* structure. The structure unit cell was divided in two layers corresponding to hydrogen and carbon atoms.The corresponding layer atom position is depicted in Fig. 2 with the corresponding number of layer.

tab:up-unitcell

III. RESULTS

sec:results

We preset the results for $|\mathcal{V}^{\rm a}(\omega,\alpha)|$ and $|\mathcal{V}_{\sigma^{\rm b}}(\omega,\alpha)|$ for the $C_{16}H_8$-alt and $C_{16}H_8$-up structures being both noncentrosymmetric semi-infinite 2D carbon systems with 50% hydrogenation in different arrangements. The *alt* system has alternating hydrogen atoms on the upper and bottom sides of the carbon sheet, while the *up* system has H only on the upper side. We take the hexagonal carbon lattice to be on the xy plane for both structures, and the carbon-hydrogen bonds on the perpendicular xz plane, as depicted in Figs. 1 and 2.

We calculated the self-consistent ground state and the Kohn-Sham states using density functional theory in the local density approximation (DFT-LDA) with a planewave basis using the ABINIT code[2]. We used Hartwigsen-Goedecker-Hutter (HGH) relativistic separable dual-space Gaussian pseudopotentials[3] including the spin-orbit interaction needed to calculate $\mu^{\rm abcd}(\omega,\alpha)$ presented in Eq. (2). The convergence parameters for the calculations of our results corresponding to the *alt* and *up* structures are cut-off energies of 65 Ha and 40 Ha, respectively. The energy eigenvalues and matrix elements for the *up* ad *alt* structures were calculated using 14452 **k** points and 8452 **k** points in the irreducible Brillouin zone (IBZ) presenting LDA energy band gaps of 0.72 eV and 0.088 eV, respectively. We notice that within DFT, the LDA is only one of other possible methods that can be used to determine the electronic structure of materials. Recent investigations on graphene show some of the differences in calculated values from several of these methods[4,5]. We note that the LDA is as good as these other approaches. It is also known that the DFT calculations predict a band gap for the material that differs from experiment. This can be corrected using other *ab initio* techniques, such as the GW approximation[6], but this calculation has a very high computational cost and is out of the scope in this paper. Even so, DFT still remains as an effective and useful tool for computing diverse properties derived from the electronic band structure.

Structure	Kind of system	Pol. Ang.	Energy [eV]	$\mathcal{V}^{\rm ab}(\omega,\alpha)$ ab	[Km/s]
up	2D	40	0.09	yz	87.16
			1.94	yz	22.22
			1.97	yz	-29.70
alt	2D	145	0.72	yz	-40.21
			0.91	yz	-32.89
CdSe	bulk	90	0.91	zz	-26.87
GaAs	bulk	90	2.31	xx	-21.62

TABLE III. Comparison of the reported maxima values of $\mathcal{V}^{\rm ab}$ for different structures and the corresponding polarization angle α and energy values.

tab:vab-str-comp

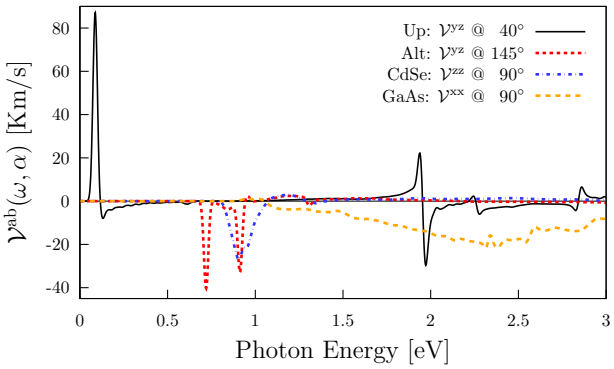

FIG. 3. Comparison of most intense responses of $\mathcal{V}^{ab}$ for 2D *alt* and *up*, and bulk CdSe and GaAs structures and the corresponding polarization angles. fig:vab-str-comp

A. Spin velocity

sec:res-spin_velocity

Using the Eq. (4), we calculated the $\mathcal{V}^{ab}(\omega,\alpha)$ response for the *alt* and *up* 2D structures and for the CdSe and GaAs bulk systems and the results are presented in Fig. 3. The angle α presented in the response of each structure is that for which the response is maximized in each case. From the figure we have that the onset of the response starts when the energy of the incoming beam is the same of the gap energy. The most intense response corresponds to the *up* structure centered at 0.088 eV corresponding to the Far Infrared (FIR) radiation and reaching a spin velocity of 87.2 Km/s. In the other hand, for an energy range from 0.66 eV to 3.0 eV, corresponding to energies of the Near Infrared (NIR) and visible radiation, all the four structures have contributions in the same order of magnitude. Starting with the 2D structures we have that the *up* structure has other two peaks centered at 1.94 eV and 1.97 eV reaching spin velocities of 22.2 Km/s and -29.7 Km/s, respectively, and the *alt* structure has two peaks centered at 0.72 eV and 0.91 eV reaching spin velocities of -40.2 Km/s and -32.9 Km/s, respectively. Then, for the bulk structures we have that the CdSe has only one intense response centered at 0.91 eV reaching a spin velocity of -26.9 Km/s, and the GaAs structure has a large and almost planar zone where the response is held reaching the maximum for an incoming beam of energy of 2.31 eV and resulting in a spin velocity of -21.6 Km/s. In table III we present the comparison of this values for the 2D and bulk structures. We found that the most intense response for the spin velocity of the *up* structure is 3.25 times more intense than CdSe and 4.03 times more intense than the GaAs bulk structures. Also, the *alt* structure has a response more intense than the bulk systems but being less intense than the corresponding to the *up* one.

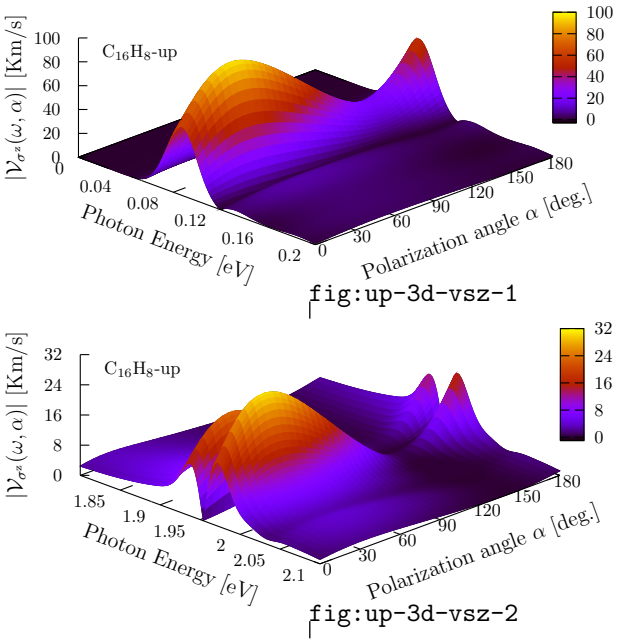

FIG. 4. $|\mathcal{V}_{\sigma^z}(\omega,\alpha)|$ response as a function of the photon energy and polarization angle α for the *up* structure for two energy ranges. The absolute maxima is located for an energy range from 0.08 eV to 0.10 eV, in the Far Infrared radiation range, and two local maxima from 1.90 eV to 1.93 eV and from 1.96 eV to 2.0 eV, in the visible radiation range, all for polarization angles between 25° and 50°. fig:up-3d-vsz

B. Fixing spin

sec:res-fixspin

Using the Eq. (6), we calculated the $|\mathcal{V}_{\sigma^b}|(\omega,\alpha)$ response and made the analysis for the case when the spin is fixed in the z direction, directed perpendicularly to the surface of the *alt* and *up* structures. Also, using the Eq. (7), we determined the angle $\gamma_b(\omega,\alpha)$ where the spin-velocity is directed on the surface of the each structure.

Up structure

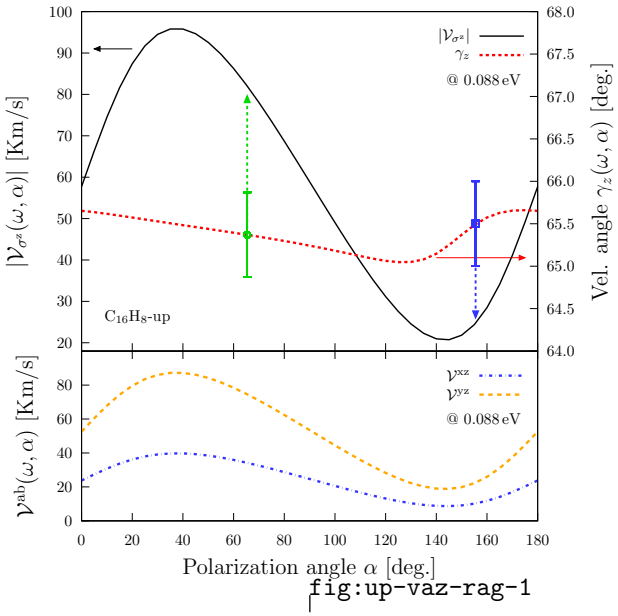

fig:up-vaz-rag-1

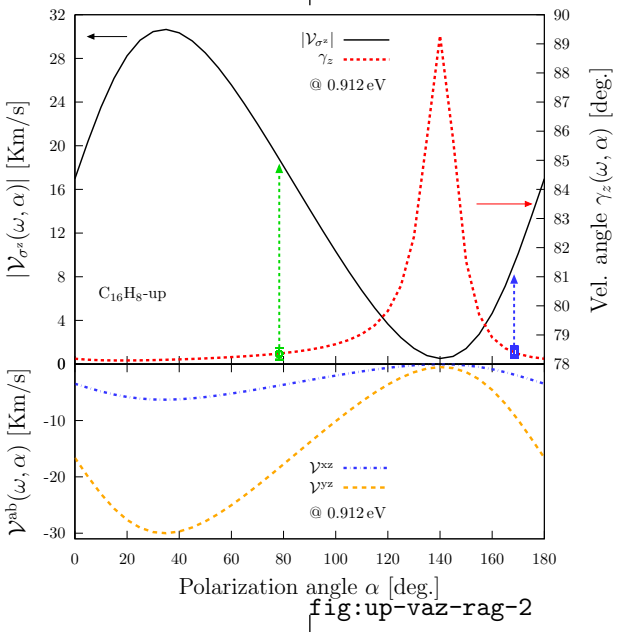

fig:up-vaz-rag-2

FIG. 5. Most intense response of $|\mathcal{V}_{\sigma^z}(\omega,\alpha)|$ (top frames, right scale of figs (a) and (b)), the corresponding velocity angle $\gamma_z(\omega,\alpha)$ (top frames, right scale), the collinear (circled box) and perpendicular (square box) angles, and the two components $\mathcal{V}^{xz}(\omega,\alpha)$ and $\mathcal{V}^{yz}(\omega,\alpha)$ (bottom frames) for the *up* structure fixing the energy to 0.088 eV.

fig:up-vaz-rag

We first analyzed two energy ranges for the *up* structure, the first for an incoming energy beam from 0.0 eV to 0.2 eV which inlude the THz and the Mid Infrared (MIR) range, where the absolute maximum of the $|\mathcal{V}_{\sigma^z}(\omega,\alpha)|$ response is obtained and the second for an energy range from 1.80 eV to 2.1 eV, corresponding to visible radiation, where two local maxima are found. In Fig. 4 we present the $|\mathcal{V}_{\sigma^z}(\omega,\alpha)|$ spectra resulting from evaluate Eq. (6) using different polarization angles α in Eq. (4). Making the analysis, we obtained that the zone where the maximum response is held corresponds to a energy range of the incident beam from 0.084 eV to 0.093 eV and polarization angles α between 30° and 45°. Also two local maxima are held for same polarization angles but for an energy range of the incoming beam between 1.90 eV and 2.05 eV. In the top frames of Figs.III B and III B we present in solid lines the result of evaluate $|\mathcal{V}_{\sigma^z}(\omega,\alpha)|$, related to the left scale, fixing the energy of the incoming beam to 0.088 eV and 0.912 eV, respectively, for which value the response is maximized for the *up* structure. In the same figures and frames we present in dashed lines, related to the right scale, the corresponding velocity angle $\gamma_z(\omega,\alpha)$ obtained from the evaluation of Eq. (7), and in the bottom frames of those figures the corresponding components $\mathcal{V}^{xz}(\omega,\alpha)$ and $\mathcal{V}^{yz}(\omega,\alpha)$. Also we present two circled and square boxes indicating the values where the angles of the spin velocity are parallel and perpendicular and the arrows are directed to the value of the response corresponding to those angles. From Figs. III B and III B we have that the absolute maximum response for the *up* structure is obtained for an incoming beam with energy of 0.088 eV and polarization angle $\alpha = 40°$ resulting in a value of $|\mathcal{V}_{\sigma^z}(\omega,\alpha)| = 95.8$ Km/s coming from the contribution of the components $\mathcal{V}^{xz}(\omega,\alpha) = 39.8$ Km/s and $\mathcal{V}^{yz}(\omega,\alpha) = 87.2$ Km/s for the spin polarized in the z direction and having a velocity angle $\gamma_z(\omega,\alpha) = 65°$ on the *xy* plane. In the same figure the green circled box indicates the value for which the polarization angle α and the response direction angle $\gamma_z(\omega,\alpha)$ are collinear being both angle 65.5° and resulting in a value of the response of $|\mathcal{V}_{\sigma^z}(\omega,\alpha)| = 82.3$ Km/s indicated by the upward green arrow. Also the blue square box indicates the value for which the polarization angle and the response angle are perpendicular being $\alpha = 155.5°$ and $\gamma_x(\omega,\alpha) = 65.5°$; for this angles the response has a value of $|\mathcal{V}_{\sigma^z}(\omega,\alpha)| = 24.8$ Km/s indicated by the blue downward arrow. The green and blue error bars

are fixed for a value of $\pm 0.5^\circ$ and then, for variations of this magnitude in $\gamma_z(\omega,\alpha)$ the complete range of α angle is included because this last is almost constant. Now from Figs. III B and III B we have that a local maxima of the response is obtained for an incoming beam with energy of 0.912 eV and same polarization angle $\alpha = 40^\circ$ resulting in a value of $|\mathcal{V}_{\sigma^z}(\omega,\alpha)| = 30.3$ Km/s. This comes from a major contribution of the $\mathcal{V}^{yz}(\omega,\alpha)$ component being directed in a velocity angle $\gamma_z(\omega,\alpha) = 78^\circ$ on the first Cartesian Quadrant of the xy plane, for the spin polarized in the z direction. Again the green circled box indicates the value for which the polarization angle α and the response direction angle $\gamma_z(\omega,\alpha)$ are collinear being both 78.5° and having a response value of $|\mathcal{V}_{\sigma^z}(\omega,\alpha)| = 23.5$ Km/s indicated with the green upward arrow. We found that for variations in the response angle of $\pm 2^\circ$, indicated with the error bars, corresponds a range in the polarization angle of $0^\circ \leq \alpha \leq 122^\circ$ having then a large range for which the direction of the response is directed to this angle. The blue square box indicates the value for which the polarization angle and the response angle are perpendicular being $\alpha = 168.5^\circ$ $\gamma_z(\omega,\alpha) = 78.5^\circ$ and having a response $|\mathcal{V}_{\sigma^z}(\omega,\alpha)| = 9.0$ Km/s indicated with the blue upward arrow. Again, for variations in the response angle of $\pm 2^\circ$, indicated with the error bars, corresponds a range in the polarization angle of $155^\circ \leq \alpha \leq 180^\circ$ having again a large range for which the direction of the response is held. The most interesting case in which the spin is perpendicular to the surface of the structure and also for the *up* structure the most intense was the presented before for which the spin is polarized in the z direction. We also made the analysis for the cases when the spin polarization is directed in the x and y direction but we do not present the corresponding plots. For those cases we have that the absolute maxima response is obtained for an energy of the incoming beam equal to 0.088 eV and polarization angle $\alpha = 40^\circ$ resulting in values of $|\mathcal{V}_{\sigma^x}(\omega,\alpha)| = 37.4$ Km/s and $|\mathcal{V}_{\sigma^y}(\omega,\alpha)| = 24.8$ Km/s.

Alt structure

For the *alt* structure we analyzed the energy range for the incident beam from 0.6 eV to 1.0 eV, corresponding to the NIR radiation, where the absolute maximum of $|\mathcal{V}_{\sigma^z}(\omega,\alpha)|$ response is obtained. In Fig. 6 we present the $|\mathcal{V}_{\sigma^z}(\omega,\alpha)|$ spectra resulting from evaluate again Eq. (6) and Eq. (4) as a function of the energy and polarization angle α of the incoming beam for the *alt* structure. From this figure we found that the zone where the absolute maxi-

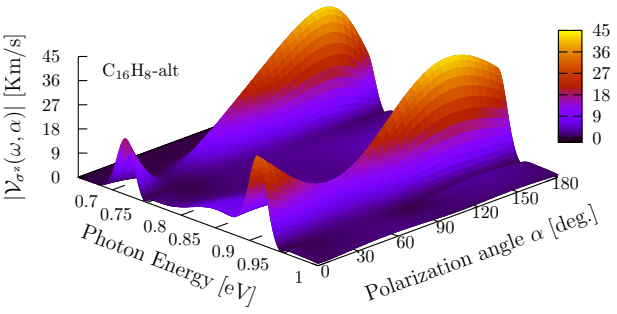

FIG. 6. $|\mathcal{V}_{\sigma^z}(\omega,\alpha)|$ response as a function of the photon energy and polarization angle α for the *alt* structure. The local and the absolute maxima are located in the energy ranges from 0.67 eV to 0.73 eV and from 0.90 eV to 0.93 eV, respectively, and both in the Near Infrared and for polarization angles between 120° and 150°. fig:alt-3d-vsb

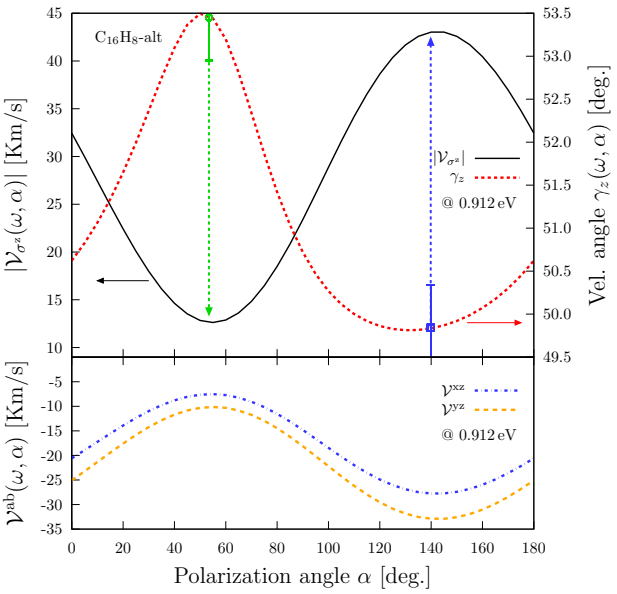

FIG. 7. Most intense response of $|\mathcal{V}_{\sigma^z}(\omega,\alpha)|$ (top frame, left scale) the corresponding velocity angle $\gamma_z(\omega)$ (top frame, right scale), the collinear (circled box) and perpendicular (square box) angles, and the two components $\mathcal{V}^{xz}(\omega)$ and $\mathcal{V}^{yz}(\omega)$ (bottom frame) for the *alt* structure fixing the energy to 0.912 eV. fig:alt-vaz-rag

mum response is held corresponds to a energy range from 0.90 eV to 0.93 eV and polarization angles α between 120° and 150°. Also, a local maximum is obtained for the same polarization angles but for energies between 0.67 eV and 0.75 eV. In the top frame of Fig. 7 we present in solid line the result of evaluate $|\mathcal{V}_{\sigma^z}(\omega,\alpha)|$, related to the left scale, fixing the energy of the incoming beam to 0.912 eV for which value the response is maximized for the *alt* structure. In the same figure and frame we present with dashed line, related to the right scale, the velocity angle $\gamma_z(\omega,\alpha)$ and in the bottom frame the corresponding $\mathcal{V}^{xz}(\omega,\alpha)$ and $\mathcal{V}^{yz}(\omega,\alpha)$ components. Again, the circled and square boxes indicate the values for which the polarization angle and the velocity angle are parallel and perpendicular and with arrows are indicated the corresponding response value. From this figure and from Fig. 6 we have that the absolute maximum response for the *alt* structure is obtained for an incoming beam with polarization angle $\alpha = 145°$ reaching a velocity of $|\mathcal{V}_{\sigma^z}(\omega,\alpha)| = 43.0$ Km/s and for the spin polarized in the z direction and resulting in a velocity angle $\gamma_z(\omega,\alpha) = 50°$ on the first Cartesian Quadrant of the xy plane. The circled box for the collinear angle corresponds for angles α and $\gamma_z(\omega,\alpha)$ equal to 53.5° with a value of $|\mathcal{V}_{\sigma^z}(\omega,\alpha)| = 12.7$ Km/s, and the blue square box indicates the perpendicular angles for values $\alpha = 140°$ and $\gamma_z(\omega,\alpha) = 50°$ with a value of $|\mathcal{V}_{\sigma^z}(\omega,\alpha)| = 43$ Km/s. Finally we found that for variations of $\pm 0.5°$ of those collinear and perpendicular angles, presented with the error bars on the boxes, correspond ranges for the polarization angle $30° \leq \alpha \leq 70°$ and $95° \leq \alpha \leq 175°$ covering a wide range of angles because the response angle $\gamma_z(\omega,\alpha)$ has small variations for the complete range of the polarization angle α. Again, for the cases in which the spin polarization is parallel to the surface of the *alt* structure was calculated but the plots are not presented here. The absolute maxima for the case when the spin polarization is directed in the x and y direction are obtained for an energy of the incoming beam equal to 0.912 eV and polarization angle $\alpha = 145°$ resulting in values of $|\mathcal{V}_{\sigma^x}(\omega,\alpha)| = 27.1$ Km/s and $|\mathcal{V}_{\sigma^y}(\omega,\alpha)| = 33.2$ Km/s.

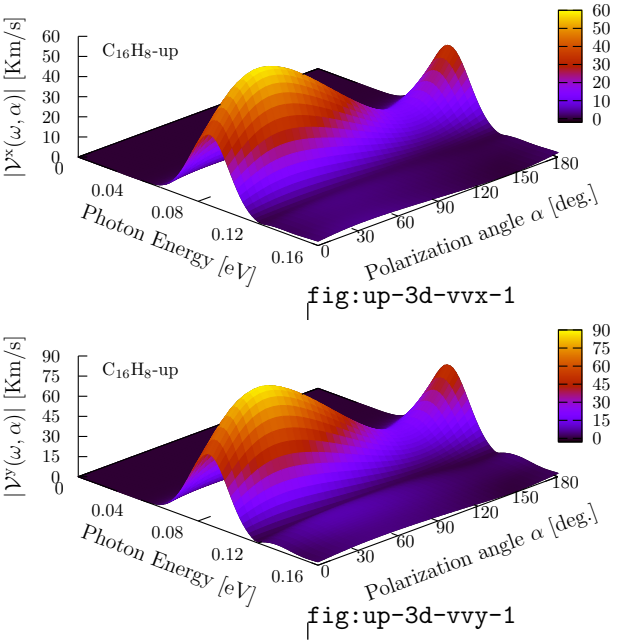

FIG. 8. $|\mathcal{V}^x(\omega,\alpha)|$ and $|\mathcal{V}^y(\omega,\alpha)|$responses as a function of the photon energy and polarization angle α for the *up* structure. The absolute maxima of both are localized in the energy range from 0.08 eV to 0.10 eV, in the Far Infrared, and for polarization angles from 25° to 50°. fig:up-3d-vva-1

C. Fixing velocity

sec:res-fixvel

Now, using the Eq. (8), we calculated the $|\mathcal{V}^a(\omega,\alpha)|$ response and made the analysis for the case when the velocity is fixed in the x and y direction over the surface of the *alt* and *up* structures. Also, using the Eqns. (9) and (10), we determined the polar $\theta_a(\omega,\alpha)$ and azimuthal $\varphi_a(\omega,\alpha)$ angles where the spin polarization is directed.

Up structure.

For the *up* structure we first analyzed the energy range from 0.00 eV to 0.16 eV, where we found the most intense response and the absolute maxima for $|\mathcal{V}^x(\omega,\alpha)|$ and $|\mathcal{V}^y(\omega,\alpha)|$ presented in Fig. 8 and resulting from evaluate Eq. (8) as a function of the polarization angle α in Eq. (4) for the *up* structure. From this picture we can see that for the zone between the energy range of 0.084 eV-0.093 eV and polarization angles between 30° and 45° is the zone where the maximum response is held for both, $|\mathcal{V}^x(\omega,\alpha)|$ and $|\mathcal{V}^y(\omega,\alpha)|$.

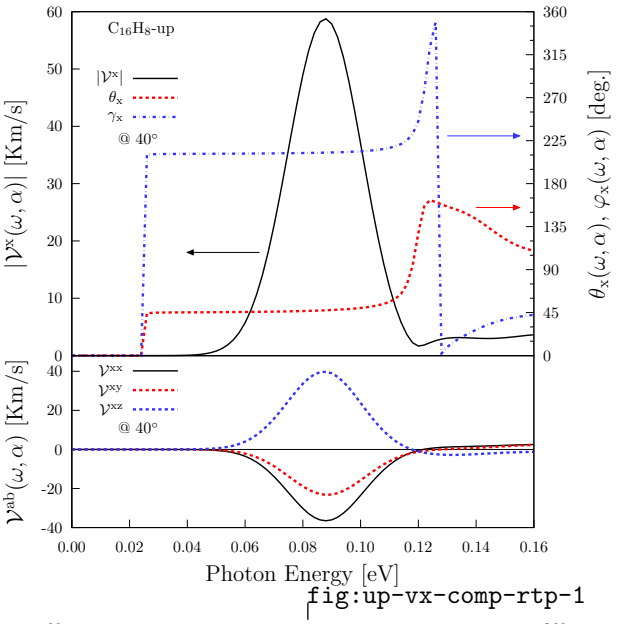

fig:up-vx-comp-rtp-1

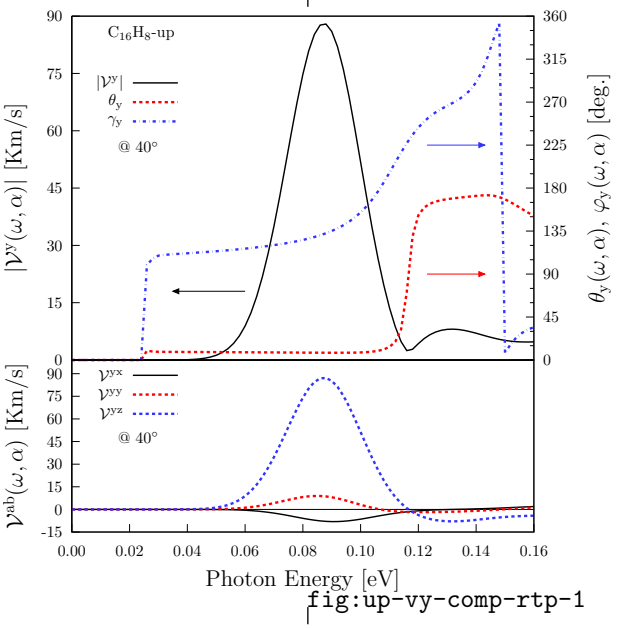

fig:up-vy-comp-rtp-1

FIG. 9. Most intense response of $|\mathcal{V}^{\rm x}(\omega,\alpha)|$ and $|\mathcal{V}^{\rm y}(\omega,\alpha)|$ (top frames left scale of Figs. (a) and (b)), the corresponding polar φ and azimuthal θ angles (top frames right scale), and the corresponding three components (bottom frames) for the *up* structure fixing the polarization angle to $\alpha = 40°$ to maximize the response.

fig:up-vab-comp-rtp-1

In the top frames of Figs. III C and III C we present in solid lines the results of $|\mathcal{V}^{\rm x}(\omega,\alpha)|$ and $|\mathcal{V}^{\rm y}(\omega,\alpha)|$, related to the left scale, fixing the polarization angle to $\alpha = 40°$ for which the response is maximized. In the same figures and frames we present in dashed lines the corresponding polar $\theta_a(\omega,\alpha)$ and azimuthal $\varphi_a(\omega,\alpha)$ angles related to the right scale. Also, in the bottom frames of those figures we present the decomposition of $|\mathcal{V}^{\rm x}(\omega,\alpha)|$ and $|\mathcal{V}^{\rm y}(\omega,\alpha)|$ in the corresponding $\mathcal{V}^{\rm xx}(\omega,\alpha)$, $\mathcal{V}^{\rm xy}(\omega,\alpha)$, $\mathcal{V}^{\rm xz}(\omega,\alpha)$, and $\mathcal{V}^{\rm yx}(\omega,\alpha)$, $\mathcal{V}^{\rm yy}(\omega,\alpha)$, $\mathcal{V}^{\rm yz}(\omega,\alpha)$ components.

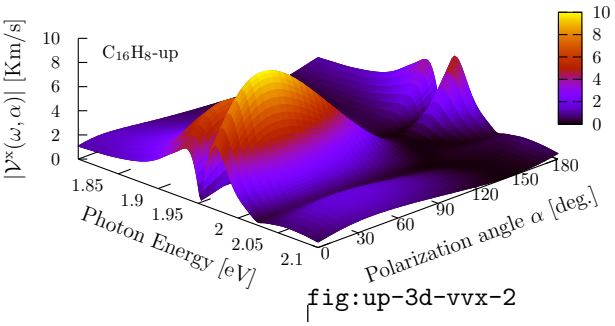

fig:up-3d-vvx-2

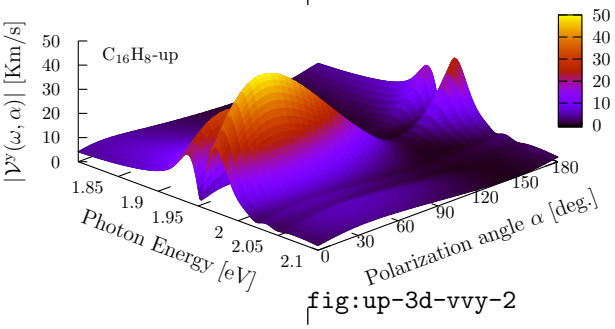

fig:up-3d-vvy-2

FIG. 10. $|\mathcal{V}^{\rm x}(\omega,\alpha)|$ (top panel) and $|\mathcal{V}^{\rm y}(\omega,\alpha)|$ (bottom panel) as a function of the photon energy and polarization angle α for the *up* structure. Two local maxima of both responses are localized in the energy range from 1.90 eV to 1.93 eV and from 1.96 eV to 2.0 eV, in the visible radiation range, and for polarization angles between 25° and 50°.

fig:up-3d-vva-2

From Fig. III C we have that for an incoming bean with energy of 0.088 eV the three components have similar contributions and with values of $\mathcal{V}^{\rm xx}(\omega,\alpha) = -36.5\,{\rm Km/s}$, $\mathcal{V}^{\rm xy}(\omega,\alpha) = -23.2\,{\rm Km/s}$, and $\mathcal{V}^{\rm xz}(\omega,\alpha) = 39.8\,{\rm Km/s}$ resulting in a value of $|\mathcal{V}^{\rm x}(\omega,\alpha)| = 58.7\,{\rm Km/s}$ being this value the absolute maximum obtained when the spin-velocity is fixed in the x direction. To this value corresponds a polar and azimuthal angles of $\theta_{\rm x}(\omega,\alpha) = 47$ and $\varphi_{\rm x}(\omega,\alpha) = 212$, respectively, being directed upper the third Cartesian Quadrant of the xy plane. Also from this figure we have that those angle values are hold for almost all the peak of the response having a deviation of $\pm 2°$ in the range of energies from 0.028 eV to 0.098 eV from the corre-

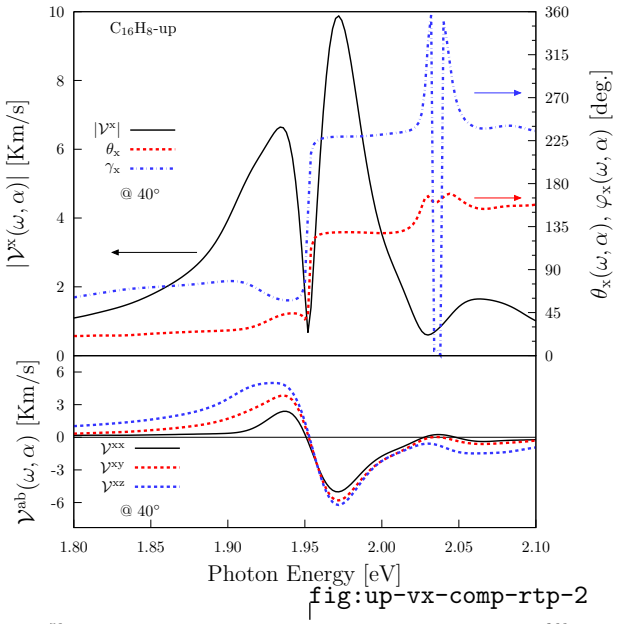

fig:up-vx-comp-rtp-2

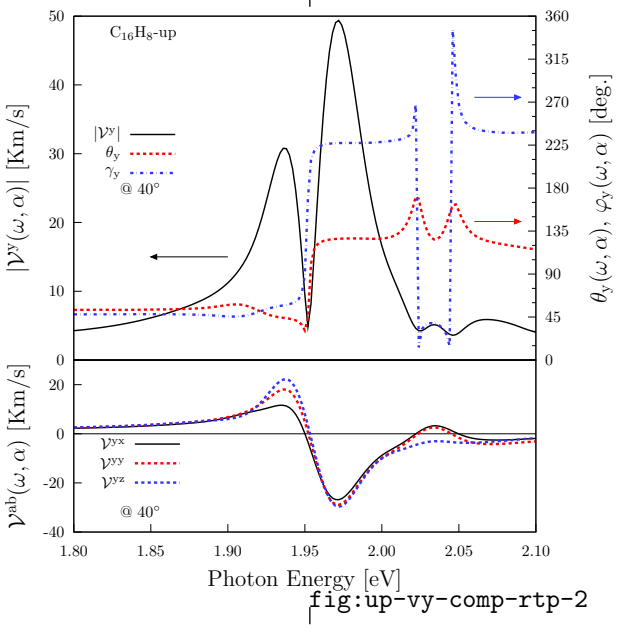

fig:up-vy-comp-rtp-2

FIG. 11. Intense response of $|\mathcal{V}^{x}(\omega,\alpha)|$ and $|\mathcal{V}^{y}(\omega,\alpha)|$ (top frames left scale of Figs. (a) and (b)), the corresponding polar φ and azimuthal θ angles (top frames right scale), and the corresponding three components (bottom frames) for the *up* structure fixing the polarization angle to $\alpha = 40°$ to maximize the response.

fig:up-vab-comp-rtp-2

sponding to the absolute maximum mentioned before. Now, from Fig. III C we have that the yx and yy components have less contributions for the total response than the yz and for the same incoming beam energy have values of $\mathcal{V}^{yx}(\omega,\alpha) = -7.9\,\mathrm{Km/s}$ $\mathcal{V}^{yy}(\omega,\alpha) = 8.6\,\mathrm{Km/s}$, and $\mathcal{V}^{yz}(\omega,\alpha) = 87.2\,\mathrm{Km/s}$ resulting in a value of the total response of $|\mathcal{V}^{y}(\omega,\alpha)| = 87.9\,\mathrm{Km/s}$ being this value the absolute maximum obtained when the spin-velocity is fixed in the y direction and being 1.5 times more intense than $|\mathcal{V}^{x}(\omega,\alpha)|$ To this absolute maximum correspond spin polar and azimuthal angles $\theta_{y}(\omega,\alpha) = 8$ and $\varphi_{y}(\omega,\alpha) = 133$, respectively, being directed almost perpendicularly over the xy plane and being localized on the first Cartesian Quadrant. In a different way than in the $|\mathcal{V}^{x}(\omega,\alpha)|$ case only the polar angle is hold for the peak of the response having a deviation of $\pm 2°$ since the onset to a energy value of 0.106 eV but the azimuthal angle changes since the onset to 0.106 eV from 99° to 176°. We also found that since the onset of the response till an energy for the incoming beam of 0.118 eV the components of both, $|\mathcal{V}^{x}(\omega,\alpha)|$ and $|\mathcal{V}^{y}(\omega,\alpha)|$ have no change in the spin polarization direction. Finally, after this energy value both goes to zero. Also there is another energy range of interest for an incoming energy beam from 1.80 eV to 2.10 eV, corresponding to the THz and visible radiation, presented in Fig. 10 where two local maxima of $|\mathcal{V}^{x}(\omega,\alpha)|$ and $|\mathcal{V}^{y}(\omega,\alpha)|$ are obtained for the *up* structure. From this figure we have that for the zone between the energy ranges from 1.92 eV to 1.94 eV and from 1.96 eV to 1.98 eV and for polarization angles from 30° to 45° those two local maxima zones are held. We found that the two local maxima are obtained for an energy of the incident beam energies of 1.934 eV and 1.972 eV fixing again the polarization angle to 40°. In the top frames of Figs. III C and III C we present in solid lines the results of $|\mathcal{V}^{x}(\omega,\alpha)|$ and $|\mathcal{V}^{y}(\omega,\alpha)|$, related to the left scale, fixing the polarization angle to $\alpha = 40°$ for which the response is maximized for the *up* structure. In the same figures and frames we present in dashed lines the corresponding polar ($\theta_{x}(\omega,\alpha)$ and $\theta_{y}(\omega,\alpha)$) and azimuthal ($\varphi_{x}(\omega,\alpha)$ and $\varphi_{y}(\omega,\alpha)$) angles related to the right scale. In the bottom frames of same figures we present the decomposition of the responses in the three corresponding components $\mathcal{V}^{xx}(\omega,\alpha)$, $\mathcal{V}^{xy}(\omega,\alpha)$, $\mathcal{V}^{xz}(\omega,\alpha)$ and $\mathcal{V}^{yx}(\omega,\alpha)$, $\mathcal{V}^{yy}(\omega,\alpha)$, $\mathcal{V}^{yz}(\omega,\alpha)$. We found that for both cases, the components have similar contributions and for an incoming energy beam of 1.934 eV we have the first local maximum resulting in a

value of $|\mathcal{V}^{\rm x}(\omega,\alpha)| = 6.6\,{\rm Km/s}$ along the x direction with polar and azimuthal spin polarization angles $\theta_{\rm x}(\omega,\alpha) = 42^\circ$ and $\varphi_{\rm x}(\omega,\alpha) = 59^\circ$ having fluctuations but being directed over the first Cartesian Quadrant of the xy plane. For the spin moving along the y direction we have a value of $|\mathcal{V}^{\rm y}(\omega,\alpha)| = 28.7\,{\rm Km/s}$ with polar and azimuthal angles $\theta_{\rm y}(\omega,\alpha) = 45^\circ$ and $\varphi_{\rm y}(\omega,\alpha) = 56^\circ$ having variations of $\pm 5^\circ$ for energy variations of $\pm 0.01\,{\rm eV}$ and being directed over the fir Cartesian Quadrant of the xy plane. Alike, for an incoming energy beam of 1.972 eV we found the second and more intense local maxima with all the components of both responses having similar contributions and resulting in values of $|\mathcal{V}^{\rm x}(\omega,\alpha)| = 9.9\,{\rm Km/s}$ and spin polarization angles $\theta_{\rm x}(\omega,\alpha) = 129^\circ$ and $\varphi_{\rm x}(\omega,\alpha) = 229^\circ$ being almost constant in the width of the peak having variations of $\pm 1^\circ$ for variations in energy of $\pm 0.01\,{\rm eV}$ and being directed downward the third Cartesian Quadrant of the xy plane. For the spin moving in the y direction we have a value of $|\mathcal{V}^{\rm y}(\omega,\alpha)| = 49.4\,{\rm Km/s}$ with spin polarization angles $\theta_{\rm y}(\omega,\alpha) = 127^\circ$ and $\varphi_{\rm y}(\omega,\alpha) = 227^\circ$ being almost constant with variations of $\pm 1^\circ$ for variations in energy of $\pm 1\,{\rm eV}$ and being directed downward the third Cartesian Quadrant of the xy plane. Finally we have that for bot energies $|\mathcal{V}^{\rm y}(\omega,\alpha)|$ is more intense than $|\mathcal{V}^{\rm x}(\omega,\alpha)|$ being 4.4 times more intense for 1.932 eV and 5.0 times more intense for 1.972 eV. Also all the components of the responses keep the spin polarization positive till an energy of the incoming beam equal to 1.954 eV when the spin polarization changes the direction and after an energy for the incoming beam equal to 2.05 eV both responses goes to zero.

Alt structure.

For the *alt* structure we analyzed the energy range from 0.6 eV to 1.0 eV, corresponding to the THz radiation, where we found the a local maxima and the most intense responses for $|\mathcal{V}^{\rm x}(\omega,\alpha)|$ and $|\mathcal{V}^{\rm a}(\omega,\alpha)|$. In Fig. 12 we present the $|\mathcal{V}^{\rm a}(\omega,\alpha)|$ spectra resulting from evaluate again Eq. (8) using different polarization angles α in Eq. (4) but now for the *alt* structure. We can see that the onset of the response is when the energy of the incoming light is the same of the gap energy. From this picture we can see that for the

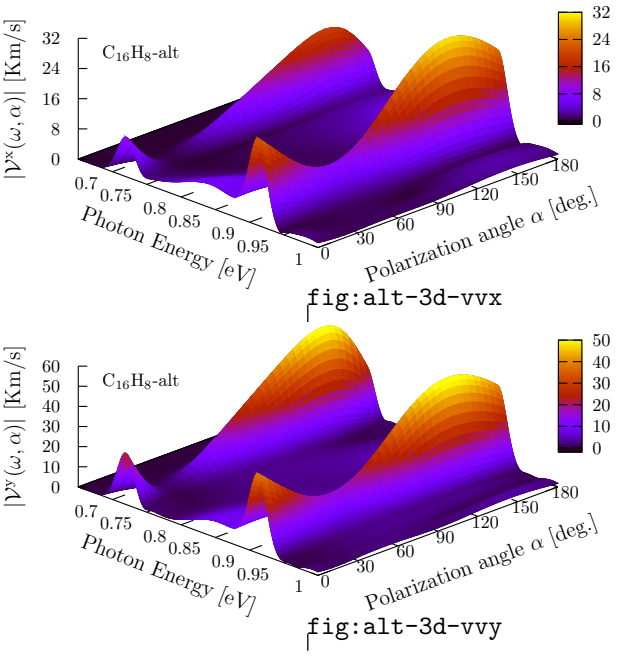

FIG. 12. $|\mathcal{V}^{\rm x}(\omega,\alpha)|$ (top panel) and $|\mathcal{V}^{\rm y}(\omega,\alpha)|$ (bottom panel) as a function of the photon energy and polarization angle α for the *alt* structure. The local and the absolute maxima are located in the energy ranges from 0.67 eV to 0.73 eV and from 0.90 eV to 0.93 eV, respectively, and both in the Near Infrared and for polarization angles between 120° and 150°. fig:alt-3d-vva

zone between the energy range of 0.90 eV-0.93 eV and polarization angles between 120° and 150° is the zone where the maximum response for both, $|\mathcal{V}^{\rm x}(\omega,\alpha)|$ and $|\mathcal{V}^{\rm y}(\omega,\alpha)|$ is held. We also found that the first peak is obtained when the energy of the incoming beam is 0.720 eV and the absolute maximum of the response is obtained when for 0.912 eV, both for a polarization angle $\alpha = 145^\circ$. In the top frames of Figs. III C and III C we present in solid lines the results of $|\mathcal{V}^{\rm x}(\omega,\alpha)|$ and $|\mathcal{V}^{\rm y}(\omega,\alpha)|$, related to the left scale, fixing the polarization angle to $\alpha = 145^\circ$ for which the response is maximized for the *alt* structure. In the same figures and frames we present ind dashed lines the spin polarization angles related to the right scale and in the bottom frames the corresponding three components. Making the analysis for the components and angles when the spin current is directed in the x direction, corresponding to the Fig. III C, we found that for the *alt* structure when the energy of the incoming beam is 0.720 eV we have similar contributions

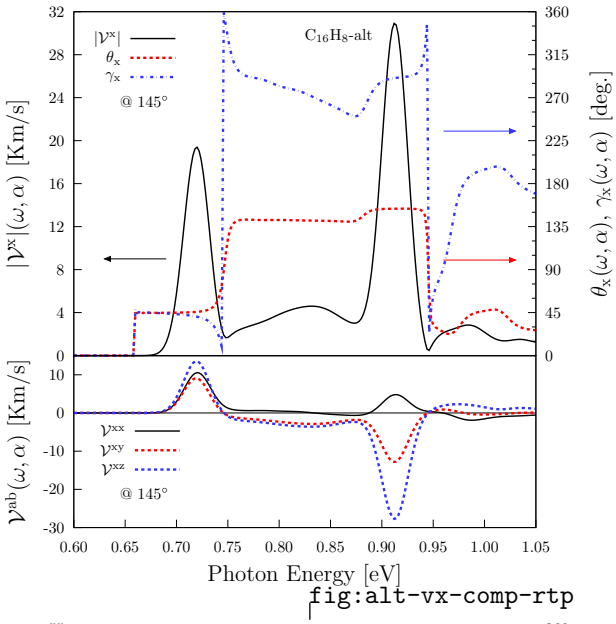

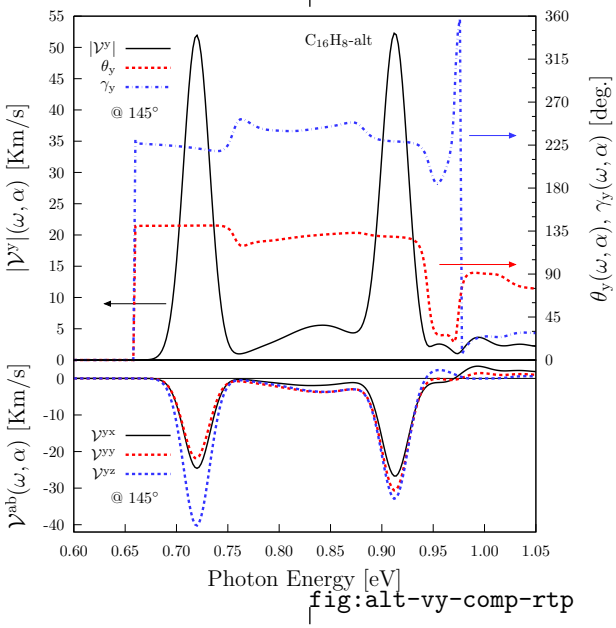

FIG. 13. Most intense response of $|\mathcal{V}^{\rm x}(\omega,\alpha)|$ and $|\mathcal{V}^{\rm y}(\omega,\alpha)|$ (top frames left scale of Figs. (a) and (b)), the corresponding polar φ and azimuthal θ angles (top frames right scale), and the corresponding three components (bottom frames) for the *alt* structure fixing the polarization angle to $\alpha = 145°$ to maximize the response.

fig:alt-vab-comp-rtp

from all the components resulting in a response of $|\mathcal{V}^{\rm x}(\omega,\alpha)| = 19.4\,{\rm Km/s}$ and polar and azimuthal spin polarization angles $\theta_{\rm x}(\omega,\alpha) = 46°$ and $\varphi_{\rm x}(\omega,\alpha) = 41°$ having variations in the range of the peak but being directed over the first Cartesian Quadrant of the xy plane; for an energy of 0.912 eV we have a major contribution from the $\mathcal{V}^{\rm xz}(\omega,\alpha)$ component resulting in a total response of $|\mathcal{V}^{\rm x}(\omega,\alpha)| = 30.9\,{\rm Km/s}$ and angles $\theta_{\rm x}(\omega,\alpha) = 154°$, and $\varphi_{\rm x}(\omega,\alpha) = 290°$ having variations of $\pm 3°$ in for energy variations of ± 1 eV and being directed downward the fourth Cartesian Quadrant of the xy plane. Making now the analysis for the components and angles when the spin current is directed along the y direction, corresponding to the Fig. III C, we found that when the energy of the incoming beam is 0.720 eV we have more contribution from the $\mathcal{V}^{\rm yz}(\omega,\alpha)$ component resulting in a response of $|\mathcal{V}^{\rm y}(\omega,\alpha)| = 51.9\,{\rm Km/s}$ and angles $\theta_{\rm y}(\omega,\alpha) = 141°$ and $\varphi_{\rm y}(\omega,\alpha) = 222°$ being the first constant and the second having variations of $\pm 3°$ for energy variations of ± 0.3 eV and being directed downward the third Cartesian Quadrant of the xy plane. Then, for the peak centered at 0.912 eV we have similar contributions of all the components resulting in a response $|\mathcal{V}^{\rm y}(\omega,\alpha)| = 52.3\,{\rm Km/s}$ being this the absolute maximum response for the *alt* structure. The corresponding angles are $\theta_{\rm y}(\omega,\alpha) = 129°$ and $\varphi_{\rm y}(\omega,\alpha) = 229°$ being both constant for the energy range of the peak and being directed downward the third Cartesian Quadrant of the xy plane. Finally we have that the three components of $|\mathcal{V}^{\rm y}|$ are negative keeping the same spin polarization since the onset of the response to a energy of the incoming beam of 0.886 eV when the response decreases and goes to zero.

IV. LAYER-BY-LAYER ANALYSIS

sec:res-layer_by_layer_analysis

The structures presented here where divided into layers to analyze the he layer-by-layer contribution for $\mathcal{V}^{\rm ab}$ response. The *alt* structure was divided in six layers corresponding the first one to the top hydrogen atoms, from the second to the forth to carbon atoms in different z positions, and the sixth and last one to the bottom hydrogen atoms. The *up* structure was divided into two layers, the first one comprised by the top hydrogen atoms and the second by the carbon atoms. The layer divisions and atom positions for the unit cells are shown in Tables I and II.

From the bottom frames of Figs. 9 and 11 we

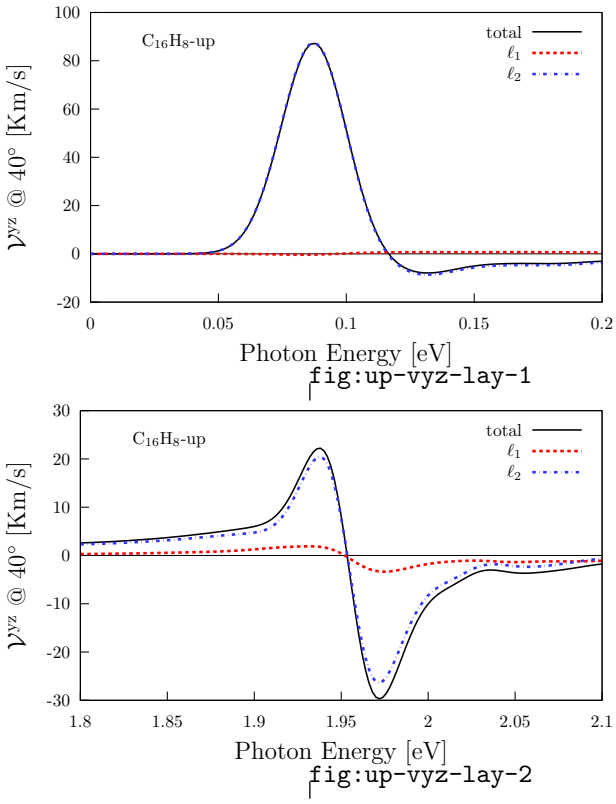

FIG. 14. Layer-by-layer contribution of $\mathcal{V}^{yz}$ for the *up* structure. fig:up-vyz-lay

can see that for the *up* structure again the most intense component of $|\mathcal{V}^{x}|$ and $|\mathcal{V}^{y}|$ corresponds to $\mathcal{V}^{yz}$ which has a value of 87.2 Km/s for an energy incident beam of 0.088 eV and -29.7 Km/s for an energy incident beam of 1.972 eV. This component and the corresponding layer by layer contribution is depicted in Fig. 14s. From this figure we have that for the energy range from 0 eV to 0.2 eV the response comes from the second layer composed by carbon atoms presented in Tab. II and denoted by the number 2 in Fig. 2. In the other hand, the response for the energy range from 1.8 eV to 2.1 eV almost all the response comes from the carbon atoms having a leaser contribution from the hydrogen layer. From the bottom frames of Fig. 13 we can see that for the *alt* structure the most intense component of $|\mathcal{V}^{x}|$ and $|\mathcal{V}^{y}|$ corresponds to $\mathcal{V}^{yz}$ which has a value of -40.2 Km/s for an energy incident beam of 0.72 eV. This component and the corresponding layer by layer contribution is depicted in Fig. 15. From this figure we have that for the energy range from 0.70 eV to 0.74 eV the fifth and sixth layers corresponding to the bottom carbon and hydrogen numbered with 5 and 6 in Fig. 1 have contributions in opposite direction than the other 4 layers resulting in a total response $\mathcal{V}^{yz} = -40.2$ Km/s for an incoming beam energy of 0.72 eV. In the other hand, for the energy range from 0.88 eV to 0.95 eV the response for the all six layers the responses are in the same direction resulting in a total response $\mathcal{V}^{yz} = -32.89$ Km/s for an incoming beam with energy of 0.912 eV.

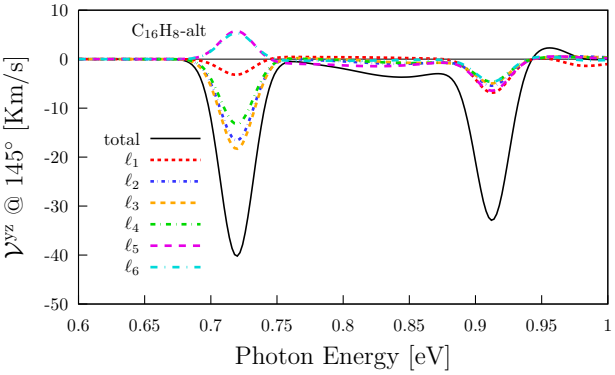

FIG. 15. Layer-by-layer contribution of $\mathcal{V}^{yz}$ for the *alt* structure. fig:alt-vyz-lay

[1] N. Arzate, R. A. Vázquez-Nava, and B. S. Mendoza, Phys. Rev. B **90**, 205310 (2014).

[2] X. Gonze, B. Amadon, P.-M. Anglade, J.-M. Beuken, F. Bottin, P. Boulanger, F. Bruneval, D. Caliste, R. Caracas, M. Côté, T. Deutsch, L. Genovese, P. Ghosez, M. Giantomassi, S. Goedecker, D. Hamann, P. Hermet, F. Jollet, G. Jomard, S. Leroux, M. Mancini, S. Mazevet, M. Oliveira, G. Onida, Y. Pouillon, T. Rangel, G.-M. Rignanese, D. Sangalli, R. Shaltaf, M. Torrent, M. Verstraete, G. Zerah, and J. Zwanziger, Comput. Phys. Commun. **180**, 2582 (2009).

[3] C. Hartwigsen, S. Goedecker, and J. Hutter, Phys. Rev. B **58**, 3641 (1998).

[4] P. Karamanis, N. Otero, and C. Pouchan, J. Phys. Chem. C **119**, 11872 (2015).

[5] A. R. Botello-Méndez, S. M. Dubois, A. Lherbier, and J. C. Charlier, Acc. Chem. Res. **47**, 3292

(2014). Phys. **74**, 601 (2002).LastBibItem
[6] G. Onida, L. Reining, and A. Rubio, Rev. Mod.